Volume 3, Number 2, 2026 Pages 1-25

Bioscience Insights

ISSN: 3080-3489 (Print)
ISSN: 3080-3497 (Online)

BioSciInsights.com

TISSUE-SPECIFIC BIOACCUMULATION OF ZN, CD, NI, FE AND CR IN THE HOUSE SPARROW (PASSER DOMESTICUS) ALONG A RURAL–URBAN GRADIENT IN DISTRICT OKARA, PUNJAB, PAKISTAN

Sadia Nazir[1], Muhammad Umair Munir[2], Ayesha Aziz[3], Muhammad Shaharyar[4], Muhammad Saleem Khan[*5]

[1,2,3,4,*5]*Department of Zoology, Faculty of Life Sciences, University of Okara, Okara, Pakistan*

[*5]samiikhan@uo.edu.pk

DOI: https://doi.org/10.5281/zenodo.22916482

Article Information

Article History

Received:	May 15, 2026
Revised:	June 27, 2026
Accepted:	August 12, 2026
Available Online:	August 31, 2026

Keywords:
Passer domesticus; biomonitoring; trace elements; cadmium; urban ecology; contamination factor; Punjab; bioindicator

Abstract

Background. *Trace-metal contamination is increasing across South Asia, but tissue-specific exposure data for urban passerines in Pakistan remain limited. The sedentary, granivorous House Sparrow (Passer domesticus) is therefore a useful sentinel of localized metal exposure.*

Objective. *To quantify zinc (Zn), cadmium (Cd), nickel (Ni), iron (Fe) and chromium (Cr) in the liver, kidney and pectoral muscle of House Sparrows occupying paired rural and urban habitats of District Okara, Punjab, and to evaluate whether the species resolves a rural–urban contamination gradient at the tissue level.*

Methods. *Bird tissues (n = 3/site) were dried, homogenized, HNO_3–H_2O_2 digested, and analysed using certified reference materials. LOD/LOQ were established from 25 procedural blanks. Site differences were assessed using Welch's t-test, Hedges' g, and BH-FDR, while CF, log_2FC, MPI, hierarchical clustering, and PCA characterized and integrated multi-element contamination patterns.*

Results. *Fourteen of the fifteen tissue × element combinations were quantifiable; Ni fell below the detection limit in kidney at both sites. Accumulation ranked Fe > Zn > Cd > Cr in kidney and Fe > Zn > Cr > Ni > Cd in liver and muscle. Every quantified element except Zn in the kidney was higher at the urban site. Enrichment was strongest for Cd (CF = 2.50 in muscle, 2.00 in kidney) and Zn (CF = 1.52 in liver, 1.50 in muscle), and weakest for Fe (CF = 1.01–1.04). MPI rose from rural to urban in all three tissues (kidney +26 %, liver +27 %, muscle +42 %). Principal component analysis separated the strata along PC1 (83.5% of variance), driven by the contrast between the Zn- and Fe-dominated kidney profile and the Fe–Cr–Ni profile of liver and muscle. After correction for multiple testing, no single contrast retained significance, a direct consequence*

of the small sample (minimum detectable effect, Cohen's d ≈ 3.1 at n = 3 per group).

Conclusions. *Metal burdens remained below published avian toxicity thresholds, indicating no acute toxicity. However, consistent changes in 13/14 contrasts, particularly for Cd, Ni, and Cr, support anthropogenic metal enrichment. P. domesticus may therefore serve as a useful sentinel of urban trace-metal exposure in central Punjab.*

1. INTRODUCTION

Heavy metals occur naturally in the Earth's crust, but industrialisation, urban expansion, intensive agriculture and waste mismanagement have restructured their biogeochemical cycling to an extent that now exceeds natural flux in many landscapes (Oladimeji et al., 2025). Zinc, lead, cadmium, nickel, chromium, copper and iron enter terrestrial systems through industrial effluent, fossil-fuel combustion, agricultural run-off, mining, refuse disposal and atmospheric deposition. Because they are neither biodegradable nor readily excreted, these elements persist in soils and sediments, partition into plant tissue and move upward through food webs, where long-term exposure can compromise both wildlife and human health (Rather et al., 2023; Zhang et al., 2021).

The toxicological picture is element-specific. Zinc is an essential cofactor in several hundred metalloenzymes, yet sustained excess produces nausea, lethargy and, importantly, secondary copper and iron deficiency through competitive interference at the intestinal mucus layer (Einhorn et al., 2024; Fosmire, 1990). Cadmium has no known biological function; it is released by fossil-fuel combustion, waste incineration, phosphate fertiliser and battery manufacture, accumulates preferentially in renal tissue, and disturbs calcium and phosphorus metabolism with downstream effects on bone mineralisation and renal function (Doccioli et al., 2024; Qu & Zheng, 2024; Sarker et al., 2022). Nickel is mobilised from rock, soil, and fossil fuels and, at elevated exposure, has been linked to impaired growth, survival, and reproduction in animals, alongside gastrointestinal, renal, and carcinogenic endpoints (Begum et al., 2022; Kumar et al., 2021). Iron is indispensable to oxygen transport and energy metabolism, but overload generates reactive oxygen species and consequent hepatic, cardiac and endocrine injury (Ali et al., 2023; Peana et al., 2022). Chromium enters the environment largely through steel and alloy production and tanning; the hexavalent form is markedly more toxic and carcinogenic than the trivalent form, with documented respiratory, hepatic, renal and neurological effects (Islam et al., 2022; Iyer et al., 2023; Wise et al., 2022).

Because direct measurement of environmental metal availability is costly and spatially coarse, biomonitoring has become the preferred route to integrated exposure assessment (Zhou et al., 2008). A bioindicator organism registers the fraction of contamination that is actually bioavailable, integrated over its foraging range and residence time, and does so at a fraction of the cost of comprehensive abiotic sampling. Plants, insects, molluscs, fish and mammals have all been deployed in this role (Maurya et al., 2019), but birds are especially informative: they are widely distributed, taxonomically well characterised, occupy several trophic levels, and accumulate contaminants in tissues that can be sampled with graded invasiveness (Eens et al., 1999; Özdemir & Azizoğlu, 2025; Panda et al., 2025).

Within Pakistan, avian biomonitoring has produced a substantial evidence base. Feathers of cattle egret (*Bubulcus ibis*) resolved spatial gradients in Pb and Cd across Punjab (Malik & Zeb, 2009), eggshells of *B. ibis* and *Egretta garzetta* recorded maternal transfer of metals in the same province (Hashmi et al., 2013), and a 48-species feather survey established that taxon, trophic level and locality jointly govern accumulation, with a national mean ranking of Fe > Zn > Cu > Pb > Mn > Cr > Ni > Co > Cd (Abbasi et al., 2015). House crow (*Corvus splendens*) feathers have since been used to compare metropolitan centres across Asia and Africa, including several Pakistani cities (Iqbal et al., 2023), while Aziz et al. (2021) documented toxic-metal burdens in birds of north-eastern Pakistan and Akram et al. (2024) reported haematological correlates of metal exposure in the Sindh Sparrow (*Passer pyrrhonotus*). Naz (2025) extended this to four passerines of central Punjab, establishing the regional baseline most directly comparable to the present work.

The House Sparrow is a particularly well-suited sentinel within this guild. It is commensal with humans, largely sedentary, granivorous, and occupies both dense urban cores and surrounding farmland, so paired sampling isolates the urbanisation contrast while holding species, diet and mobility approximately constant. Swaileh and Sansur (2006) first demonstrated that urban sparrows carry significantly higher Cu, Pb and Zn than rural conspecifics, and Albayrak and Mor (2011) confirmed tissue-dependent partitioning between polluted and reference sites in Türkiye. Subsequent work has linked metal burden to morphometric change (Albayrak & Pekgöz, 2021) and to ecologically relevant behavioural deficits at sublethal Pb (Di Liberto et al., 2024). A recent series from Meknes, Morocco, has systematically mapped Zn, Pb and Cd across blood, liver, kidney and feathers along an urban–industrial–rural gradient (Haddadi, Chahlaoui, Taouraout, Belkhiri, et al., 2024; Haddadi, Chahlaoui, Taouraout, & Ichennarn, 2025; Haddadi, Chahlaoui, Taouraout, et al., 2025; Haddadi, Chahlaoui, Taouraout, Ichennarn, et al., 2025), while Ding et al. (2023) provided comparable tissue-distribution data for the congeneric Tree Sparrow (*Passer montanus*).

Despite this body of work, tissue-resolved multi-element data for *P. domesticus* from the agricultural heartland of Punjab remain absent. District Okara is an intensively farmed landscape with a rapidly expanding urban centre, combining fertiliser and pesticide inputs, an increasing vehicle fleet and unregulated solid-waste disposal, yet its wildlife exposure profile is undescribed. The present study therefore quantifies Zn, Cd, Ni, Fe and Cr in liver, kidney and pectoral muscle of House Sparrows from paired rural and urban sites in Okara, with three specific objectives: (i) to characterise the tissue-specific accumulation hierarchy of each element; (ii) to test whether the rural–urban contrast is detectable and, if so, which elements carry the signal; and (iii) to place the measured burdens against published avian toxicity thresholds so that ecological relevance, rather than statistical significance alone, can be judged.

2. Materials and Methods

2.1 Study area

District Okara lies in the central Punjab plain at 30.8014° N, 73.4483° E, bounded by Bahawalnagar to the south, Pakpattan to the south-west, Sahiwal to the west, Faisalabad to the north, Nankana Sahib to the near-east and far-north, Kasur to the south-east, and the Indian Punjab across the international border (Government of the Punjab, n.d.). The district is a canal-irrigated agricultural belt best known for potato and maize production. Two sampling strata were defined *a priori*. The rural stratum comprised cultivated farmland and associated settlements with no industrial activity, characterised by agrochemical inputs and low traffic density. The urban stratum comprised the built-up core of Okara city, characterised by high vehicular density, roadside commerce, workshop activity and open municipal waste accumulation. Strata were separated by more than 10 km, which exceeds the routine daily movement range of sedentary House Sparrows and therefore treats the two populations as effectively independent with respect to local exposure.

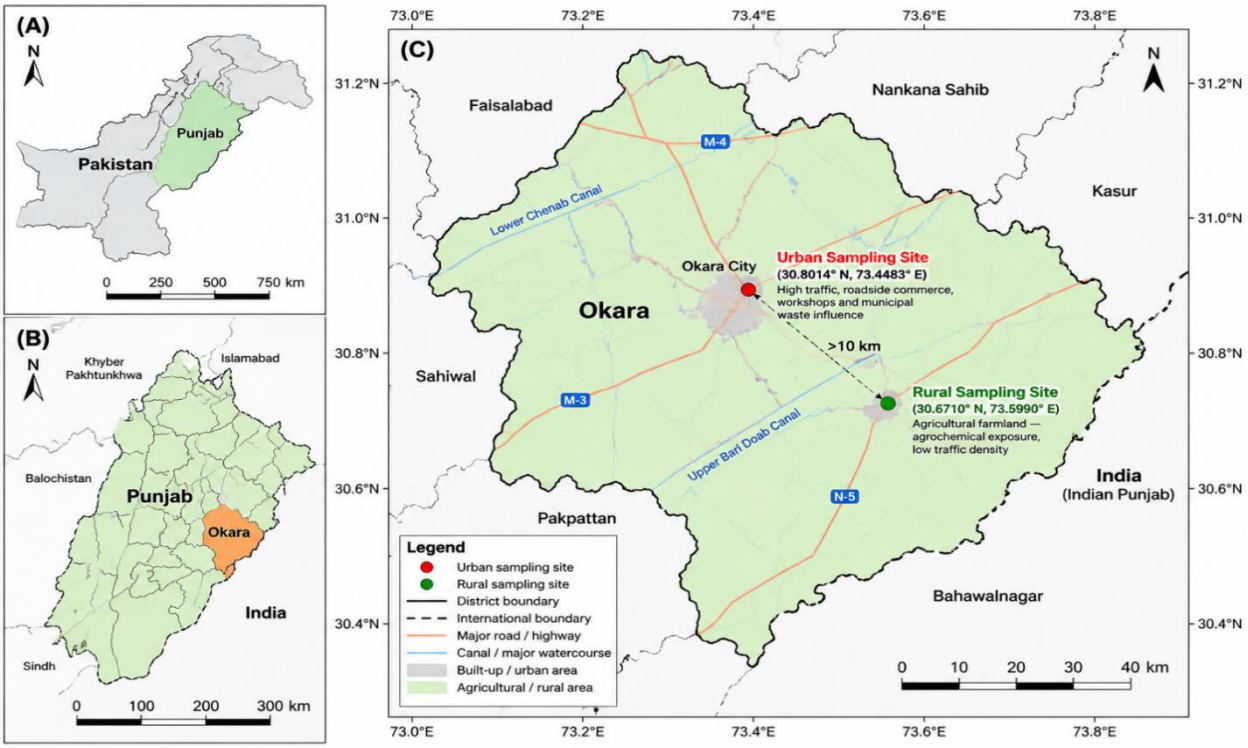


Figure 1: Map of District Okara showing the rural and urban sampling locations.

2.2 Sampling design and ethical statement

Three adult House Sparrows were obtained from each stratum (total n = 6; 18 tissue samples). Sampling was restricted to adults to avoid the age-dependent accumulation gradients reported for passerines (Ding et al., 2023; Swaileh & Sansur, 2006). Birds were dispatched humanely, and liver, kidney and pectoral muscle were excised with acid-washed stainless-steel instruments, rinsed in deionised water, placed in pre-cleaned polyethylene containers and transported chilled to the laboratory. All procedures followed institutional guidelines of the Department of Zoology, University of Okara.

2.3 Sample preparation and digestion

Tissues were dried in a forced-air oven (Heating Drying Oven IM-30) at 60 °C for 48 h to constant mass and ground to a homogeneous powder. All concentrations are therefore expressed on a dry-weight basis (μg g^{-1} dw). A 1.000 g aliquot of each homogenate was digested with 2.5 mL concentrated HNO_3 (65 %, analytical grade) and 0.5 mL H_2O_2 (30 %) on a magnetic hotplate at 200 °C until a clear, colourless digestate was obtained, following the protocol of Ding et al. (2023). Digestates were cooled, made up to 25 mL with ultrapure deionised water, and filtered prior to analysis. We used acid-washed borosilicate glassware and PTFE vessels throughout, and all reagents were analytical or trace-metal grade.

2.4 Elemental quantification

We quantified concentrations of Zn, Cd, Ni, Fe, and Cr in the digested samples using inductively coupled plasma mass spectrometry (ICP-MS). The instrument was calibrated using a five-point matrix-matched multi-element calibration series prepared by serial dilution of certified 1000 mg L^{-1} stock standards in 2% HNO_3. Calibration curves were considered acceptable when the coefficient of determination (R^2) exceeded 0.999. Procedural blanks and calibration verification standards were included throughout each analytical batch to assess contamination, instrumental stability, and analytical drift. We performed calibration verification after every ten samples, and repeated the analytical run whenever measured drift exceeded 10%. Element concentrations obtained from the instrument were subsequently corrected for the sample dilution factor and expressed relative to the original sample mass.

2.5 Quality assurance and quality control

Quality assurance and quality control procedures were implemented throughout sample digestion and elemental analysis to ensure analytical accuracy, precision, and reliability. Analytical accuracy was evaluated using NIST Standard Reference Material 1570, which was processed and analysed alongside the study samples. We subjected 25 procedural blanks to the complete digestion and analytical procedure to assess potential contamination and determine method detection limits. The limit of detection (LOD) and limit of quantification (LOQ) for each element were calculated as three and ten times, respectively, the standard deviation of the procedural blank measurements. The resulting LOD values were 0.50, 0.005, 0.006, 0.029, and 1.0 μg g^{-1} for Zn, Cd, Ni, Cr, and Fe, respectively, while the corresponding LOQ values were 1.60, 0.015, 0.019, 0.098, and 3.80 μg g^{-1}. Analytical repeatability was assessed using replicate measurements, with an acceptance criterion of ≤1% relative standard deviation (RSD); measurements exceeding this threshold were repeated. Concentrations below the corresponding LOD were reported as not detected (ND) and were excluded from ratio-based calculations rather than being replaced with arbitrary values, following recommended procedures for censored environmental data (Helsel, 2012). The instrumental operating conditions, including the analytical wavelength, fuel-flow rate, and bandpass used for each target element, are presented in **Table 1**..

Table 1. Instrumental operating conditions for the elements analysed.

Element	Wavelength (nm)	Fuel flow rate (L min^{-1})	Bandpass (nm)
Zn	213.9	0.8–1.0	0.2
Fe	248.3	0.8–1.0	0.2
Cd	228.8	1.0–1.3	0.5
Ni	232.0	0.8–1.1	0.2
Cr	357.9	2.0–3.0	0.7

2.6 Derived contamination indices

To convert raw concentrations into comparable exposure metrics, four indices were computed for every element–tissue combination. The contamination factor expresses urban enrichment relative to the rural reference:

$CF = C_{urban} / C_{rural}$

with CF ≈ 1 indicating no enrichment and CF ≥ 1.5 indicating marked enrichment. The equivalent symmetric measure, the $\log_2$ fold change ($\log_2 FC = \log_2 CF$), was used for graphical display so that depletion and enrichment occupy equal visual space.

The Metal Pollution Index integrates the multi-element burden of a tissue as the geometric mean of its constituent concentrations (Usero et al., 1997):

$MPI = (C_1 \times C_2 \times \ldots \times C_n)^{1/n}$

The geometric form prevents a single high-abundance element, here Fe — from dominating the index. Finally, we expressed the relative elemental composition of each tissue as the percentage share of the summed measured burden, providing a concentration-independent description of the exposure fingerprint.

2.7 Statistical analysis

Descriptive statistics were expressed as mean ± standard deviation. Rural–urban differences were assessed using Welch's unequal-variance *t*-test with Satterthwaite-approximated degrees of freedom, and effect sizes were reported as Hedges' *g* with 95% confidence intervals. To control for multiple comparisons, *p-values* were adjusted using the Benjamini–Hochberg false discovery rate procedure ($q < 0.05$). We further explored multivariate patterns in elemental concentrations using hierarchical clustering and principal component analysis on *z*-scored, $\log_{10}$-transformed data. All analyses were performed in Python 3 using NumPy, SciPy, pandas, and scikit-learn, and figures were prepared in Matplotlib. **Figure 2** illustrates the overall analytical workflow, from field sampling to elemental quantification and statistical analysis.

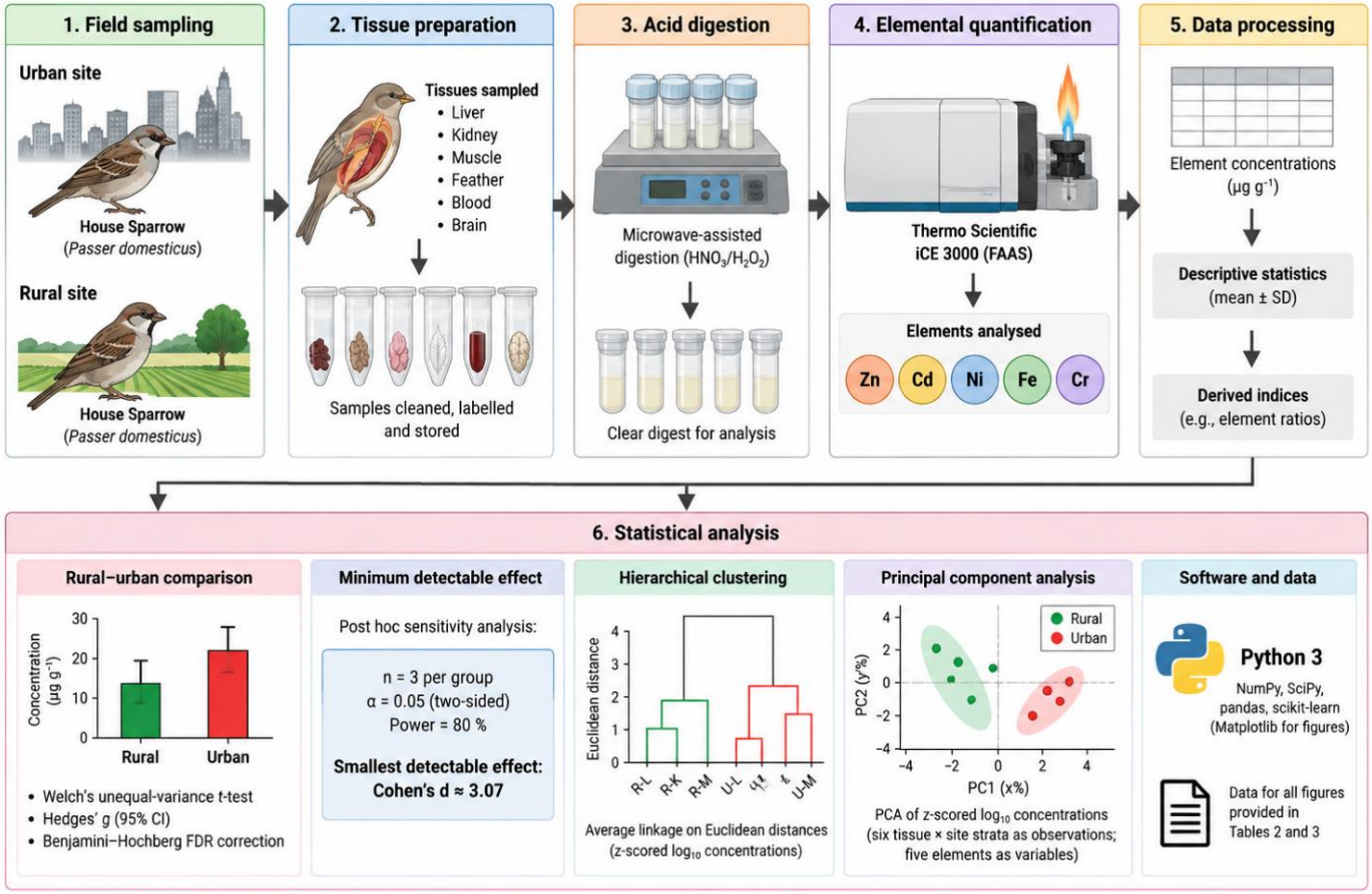


Figure 2: Analytical workflow, from field sampling through digestion and quantification to the derived-index and multivariate analyses.

3. Results

3.1 Tissue-specific elemental burden

Fourteen of the fifteen element × tissue combinations were quantifiable. Nickel fell below the limit of detection in kidney tissue at both sites and is reported as ND throughout. In kidney, Zn was the only element marginally higher in rural birds (1.04 ± 0.02 µg g^{-1}) than urban birds (1.02 ± 0.02 µg g^{-1}). Cadmium doubled from rural (0.04 ± 0.02) to urban (0.08 ± 0.01 µg g^{-1}), Fe was essentially unchanged (1.44 ± 0.03 versus 1.46 ± 0.02 µg g^{-1}), and Cr rose modestly (0.04 ± 0.02 to 0.05 ± 0.02 µg g^{-1}). The renal accumulation hierarchy was Fe > Zn > Cd > Cr. In liver, every element was higher in urban birds: Zn 0.25 ± 0.04 → 0.38 ± 0.04, Cd 0.04 ± 0.02 → 0.05 ± 0.02, Ni 0.14 ± 0.03 → 0.19 ± 0.05, Fe 4.40 ± 0.24 → 4.57 ± 0.03 and Cr 0.28 ± 0.04 → 0.34 ± 0.03 µg g^{-1}. The hepatic hierarchy was Fe > Zn > Cr > Ni > Cd. Pectoral muscle reproduced the hepatic pattern: Zn 0.26 ± 0.03 → 0.39 ± 0.02, Cd 0.02 ± 0.01 → 0.05 ± 0.01, Ni 0.14 ± 0.04 → 0.18 ± 0.02, Fe 4.39 ± 0.21 → 4.50 ± 0.02 and Cr 0.25 ± 0.03 → 0.29 ± 0.03 µg g^{-1}, giving the same hierarchy, Fe > Zn > Cr > Ni > Cd. Taken across all three tissues, 13 of the 14 quantifiable contrasts moved in the same direction — upward at the urban site. Under a null hypothesis of no habitat effect, a directional concordance this strong is itself improbable (two-sided sign test, p = 0.0018), and this collective consistency constitutes stronger evidence than any individual comparison.

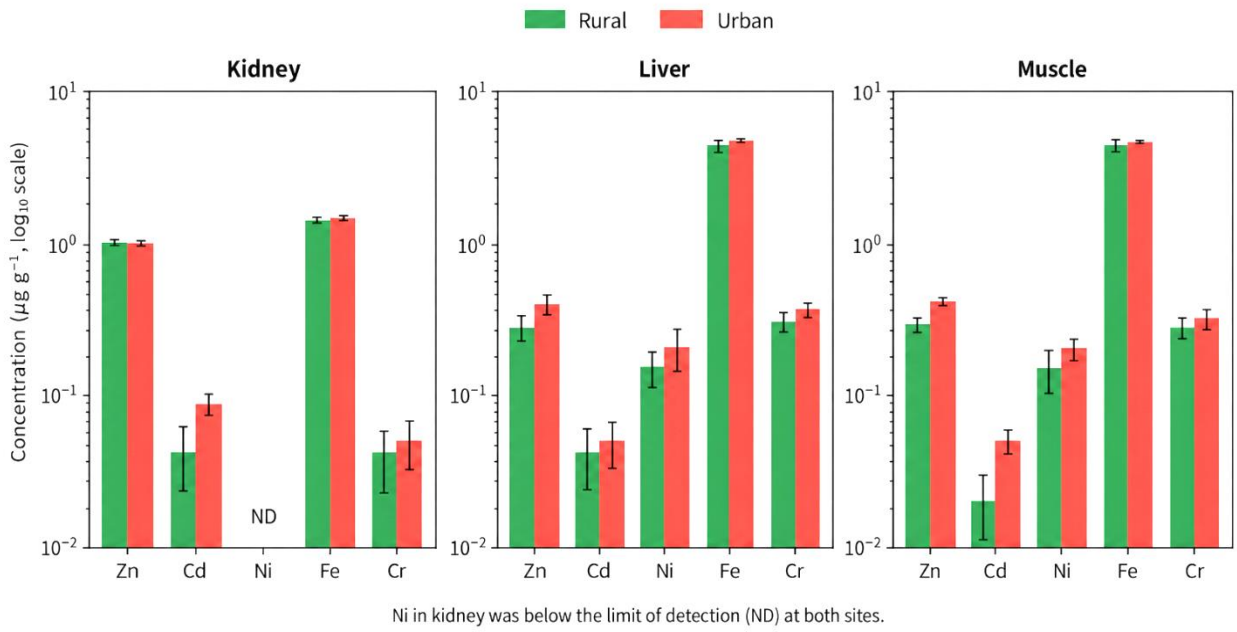


Figure 3: Tissue-specific metal burden (mean ± SD, log_{10} scale) in rural and urban House Sparrows across kidney, liver and muscle.

Table 2. Elemental concentrations (μg g^{-1} dry weight, mean ± SD; *n* = 3 per group) with re-derived inferential statistics.

Tissue	Element	Rural	Urban	*t*	df	*p*	*q* (BH)	Hedges' *g* [95 % CI]
Kidney	Zn	1.04 ± 0.02	1.02 ± 0.02	−1.22	4.00	0.288	0.448	−0.80 [−2.49, 0.89]
	Cd	0.04 ± 0.02	0.08 ± 0.01	3.10	2.94	0.055	0.192	2.02 [−0.10, 4.15]
	Ni	ND	ND	–	–	–	–	–
	Fe	1.44 ± 0.03	1.46 ± 0.02	0.96	3.48	0.399	0.507	0.63 [−1.03, 2.29]
	Cr	0.04 ± 0.02	0.05 ± 0.02	0.61	4.00	0.573	0.573	0.40 [−1.22, 2.02]
Liver	Zn	0.25 ± 0.04	0.38 ± 0.04	3.98	4.00	0.016	0.100	2.60 [0.19, 5.01]
	Cd	0.04 ± 0.02	0.05 ± 0.02	0.61	4.00	0.573	0.573	0.40 [−1.22, 2.02]
	Ni	0.14 ± 0.03	0.19 ± 0.05	1.49	3.27	0.227	0.397	0.97 [−0.77, 2.71]
	Fe	4.40 ± 0.24	4.57 ± 0.03	1.22	2.06	0.344	0.482	0.80 [−0.90, 2.49]
	Cr	0.28 ± 0.04	0.34 ± 0.03	2.08	3.71	0.112	0.313	1.36 [−0.50, 3.21]
Muscle	Zn	0.26 ± 0.03	0.39 ± 0.02	6.25	3.48	0.005	0.073	4.08 [0.83, 7.33]
	Cd	0.02 ± 0.01	0.05 ± 0.01	3.67	4.00	0.021	0.100	2.40 [0.09, 4.71]
	Ni	0.14 ± 0.04	0.18 ± 0.02	1.55	2.94	0.221	0.397	1.01 [−0.74, 2.76]

	Fe	4.39 ± 0.21	4.50 ± 0.02	0.90	2.04	0.460	0.537	0.59 [−1.06, 2.24]
	Cr	0.25 ± 0.03	0.29 ± 0.03	1.63	4.00	0.178	0.397	1.07 [−0.70, 2.83]

3.2 Multivariate structure of the exposure signal

Hierarchical clustering of the *z*-scored $\log_{10}$ concentration matrix separated the six strata into two primary clusters that corresponded to organ identity rather than to sampling site (Figure 4). Both kidney strata formed one cluster, distinguished by comparatively high Zn and low Fe; liver and muscle formed the second, distinguished by high Fe, Cr and Ni. Within the second cluster, the two urban strata grouped together and separated from their rural counterparts, indicating that the habitat signal, while secondary to organ physiology, is nonetheless resolvable. Principal component analysis recovered the same architecture in quantitative form (Figure 12). PC1 accounted for 83.5 % of total variance and PC2 for a further 15.4 %, so the first two components jointly described 98.9 % of the structure. PC1 was loaded positively by Fe, Cr and Ni and negatively by Zn, separating the kidney strata on the negative axis from the liver and muscle strata on the positive axis. PC2 was dominated by Cd and separated urban from rural strata within each organ group, with Kid·U and Liv·U/Mus·U displaced toward negative PC2 relative to their rural counterparts. Cadmium therefore emerges as the principal discriminator of habitat once organ-driven variance is partitioned out.

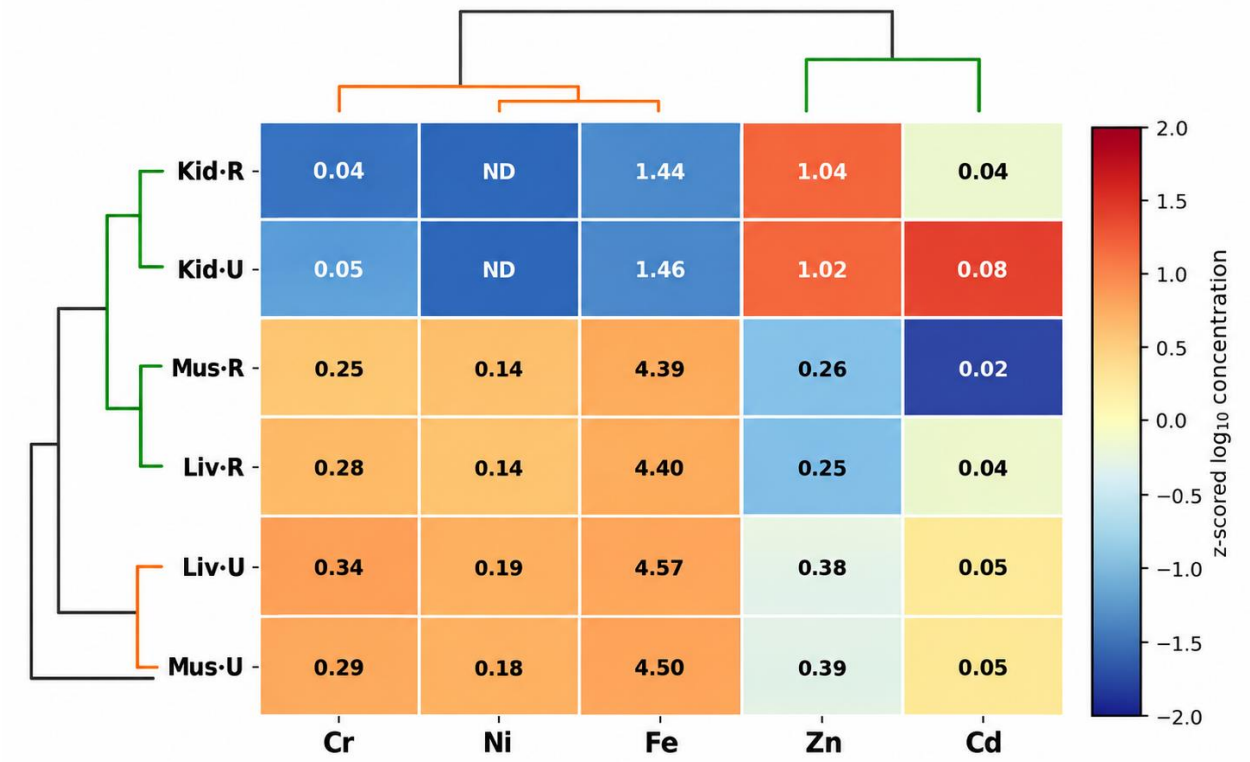


Figure 4: Hierarchical clustering heatmap of *z*-scored $\log_{10}$ concentrations across the six tissues × site strata. Cell annotations give the underlying concentration in µg g^{-1}.

3.3 Magnitude and direction of urban enrichment

Table 3 summarises contamination factors, and Figures 5, 10, and 13 show them. Enrichment was strongly element-dependent and ordered almost exactly by biological essentiality. The non-essential elements showed the largest displacement: **Cd** reached CF = 2.50 in muscle and 2.00 in kidney, equivalent to $\log_2$FC of +1.32 and +1.00. **Ni** reached CF = 1.36 (liver) and 1.29 (muscle), and **Cr** CF = 1.21–1.25 across tissues. Among the essential elements, **Zn** showed substantial enrichment in the two peripheral tissues (CF = 1.52 liver, 1.50 muscle) but none in the kidney (CF = 0.98), while **Fe** was almost invariant

across the gradient (CF = 1.01–1.04) in every tissue. The volcano representation (Figure 5) makes the pattern explicit: the three contrasts that combine a biologically meaningful fold change ($|\log_2 FC| > 0.58$) with $p < 0.05$ — Zn·muscle, Zn·liver and Cd·muscle — all fall in the urban-enriched quadrant, and no contrast falls in the rural-enriched quadrant. Cd·kidney lies immediately below the significance threshold ($p = 0.055$) despite the largest kidney fold change, a result attributable to sample size rather than to a weak signal. Effect sizes were correspondingly large (Figure 9). Hedges' g exceeded 2.0 for four contrasts (Zn·muscle $g = 4.08$; Liv·Zn $g = 2.60$; Mus·Cd $g = 2.40$; Kid·Cd $g = 2.02$) and exceeded 0.8, the conventional "large" threshold, for nine of the fourteen. Only kidney Zn produced a negative effect. Confidence intervals were wide throughout, which is the expected consequence of $n = 3$ and is discussed in Section 4.5.

Table 3. Contamination factor (CF), $\log_2$ fold change, and percentage change for each element × tissue contrast, ordered by magnitude of enrichment.

Rank	Tissue	Element	CF	$\log_2$FC	Change (%)	Interpretation
1	Muscle	Cd	2.50	+1.32	+150	Marked enrichment
2	Kidney	Cd	2.00	+1.00	+100	Marked enrichment
3	Liver	Zn	1.52	+0.60	+52	Marked enrichment
4	Muscle	Zn	1.50	+0.59	+50	Marked enrichment
5	Liver	Ni	1.36	+0.44	+36	Moderate enrichment
6	Muscle	Ni	1.29	+0.36	+29	Moderate enrichment
7	Kidney	Cr	1.25	+0.32	+25	Moderate enrichment
8	Liver	Cd	1.25	+0.32	+25	Moderate enrichment
9	Liver	Cr	1.21	+0.28	+21	Moderate enrichment
10	Muscle	Cr	1.16	+0.21	+16	Slight enrichment
11	Liver	Fe	1.04	+0.05	+4	No enrichment
12	Muscle	Fe	1.03	+0.04	+3	No enrichment
13	Kidney	Fe	1.01	+0.02	+1	No enrichment
14	Kidney	Zn	0.98	−0.03	−2	No enrichment

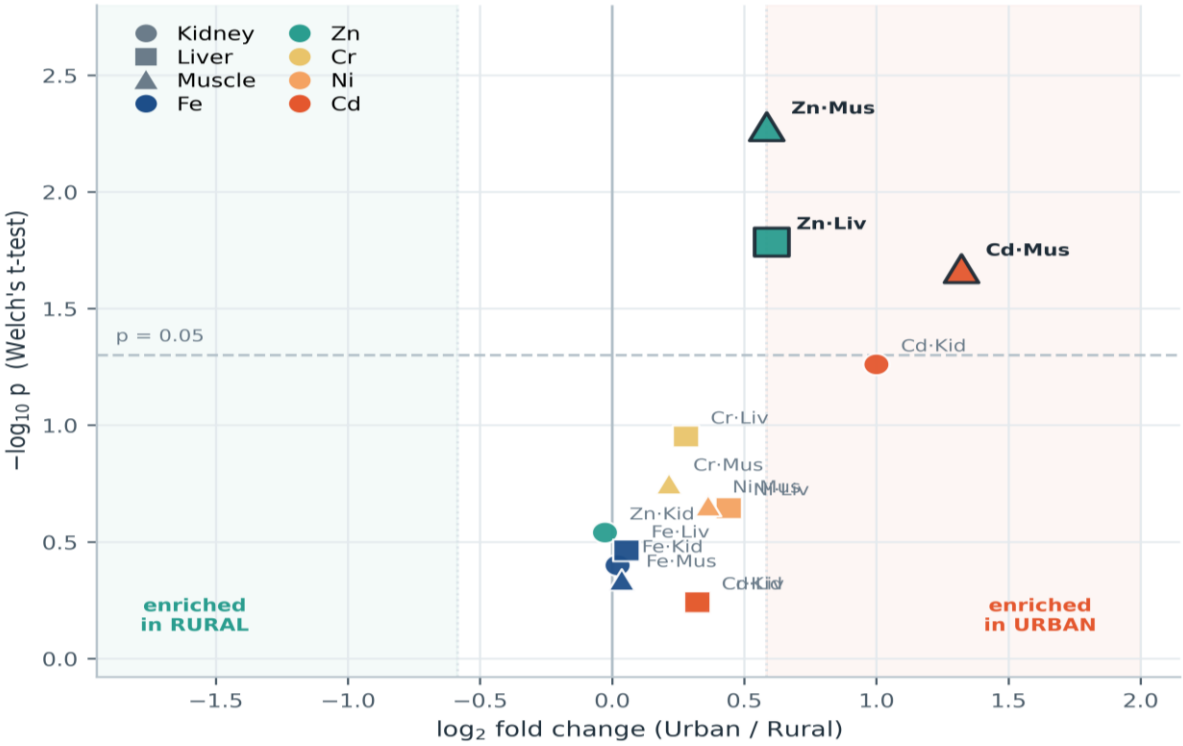


Figure 5: Volcano plot of the fourteen tissue × element contrasts. Points combining $|\log_2 FC| > 0.58$ with $p < 0.05$ are labelled in bold; all lie in the urban-enriched quadrant.

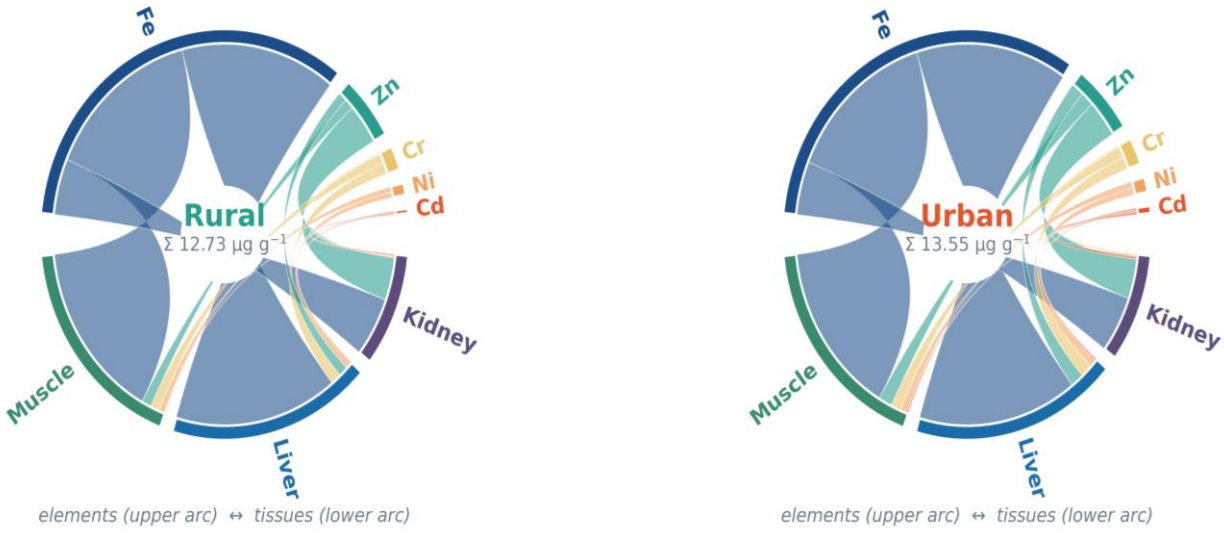


Figure 6: Chord diagram of element–tissue partitioning at the rural and urban sites; ribbon width is proportional to concentration.

3.4 Elemental fingerprints and accumulation hierarchy

The chord representation (Figure 6) and the radar profiles (Figure 7) show that the exposure fingerprint is conserved in shape but inflated in magnitude at the urban site. Iron dominated the total measured burden in every stratum, contributing 86–87 % of the summed mass in rural liver and muscle and 83 % in their urban counterparts, and 56 % in kidney at both sites (Figure 11). The apparent *decline* in Fe share at the urban site is not a decline in Fe itself — Fe concentration rose slightly in all three tissues — but a

dilution effect produced by the disproportionate rise of Cd, Ni, Cr and Zn. This is a useful diagnostic: a contamination signal driven by external inputs should expand the non-essential fraction of the fingerprint while leaving the homeostatically buffered fraction approximately constant, which is precisely what was observed. Ranking each stratum's elements from highest to lowest (Figure 8) shows that the rank order is invariant to site: kidney follows Fe > Zn > Cd > Cr and liver and muscle both follow Fe > Zn > Cr > Ni > Cd, whether birds were sampled in farmland or in the city. Habitat shifts the elevation of the curve, particularly at the low-abundance tail where Cd sits, without reordering it.

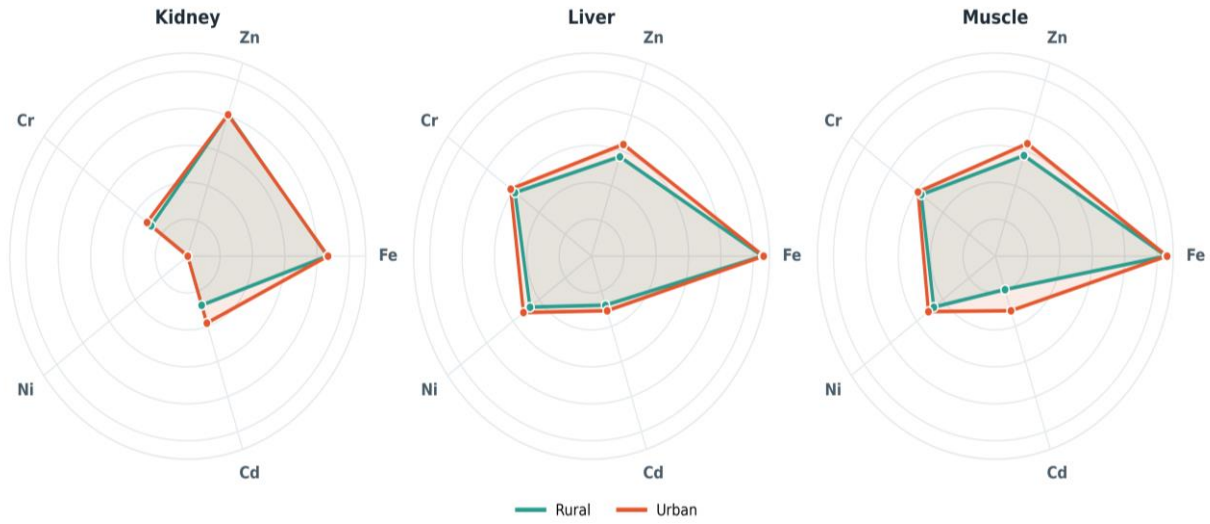


Figure 7: Radial multi-element signature of each tissue, rural versus urban (radial axis $\log_{10}$-scaled).

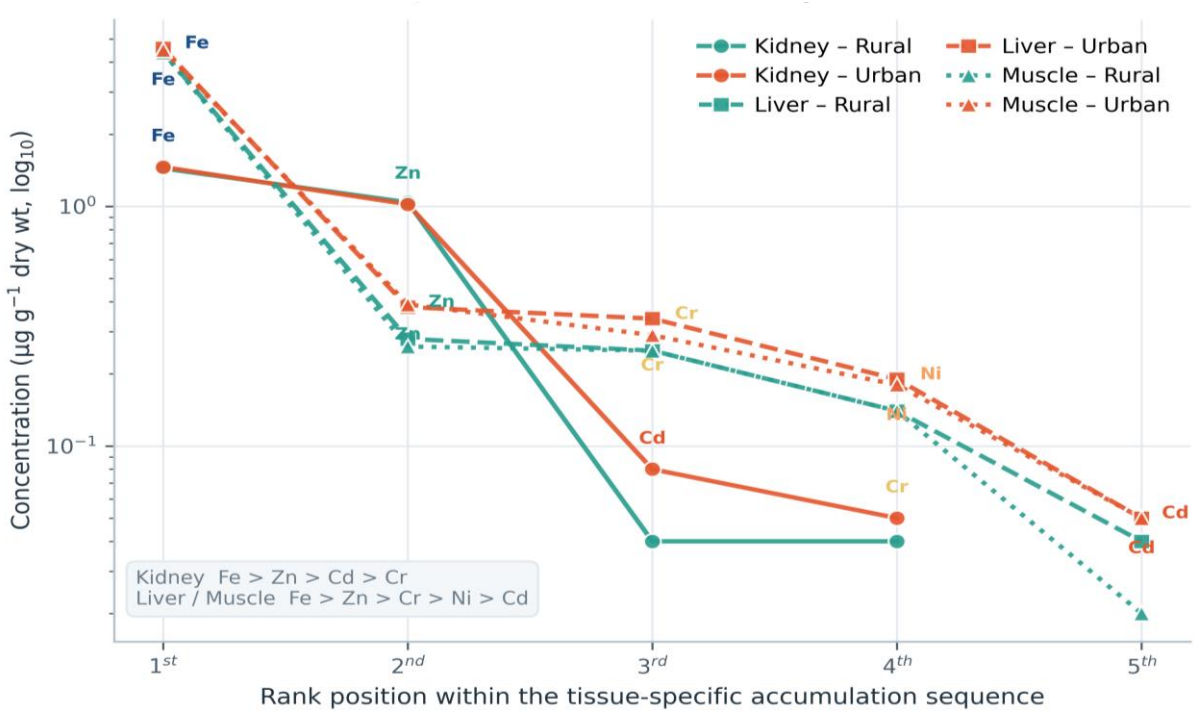


Figure 8: Rank-ordered descending accumulation profiles for each tissue × site stratum.

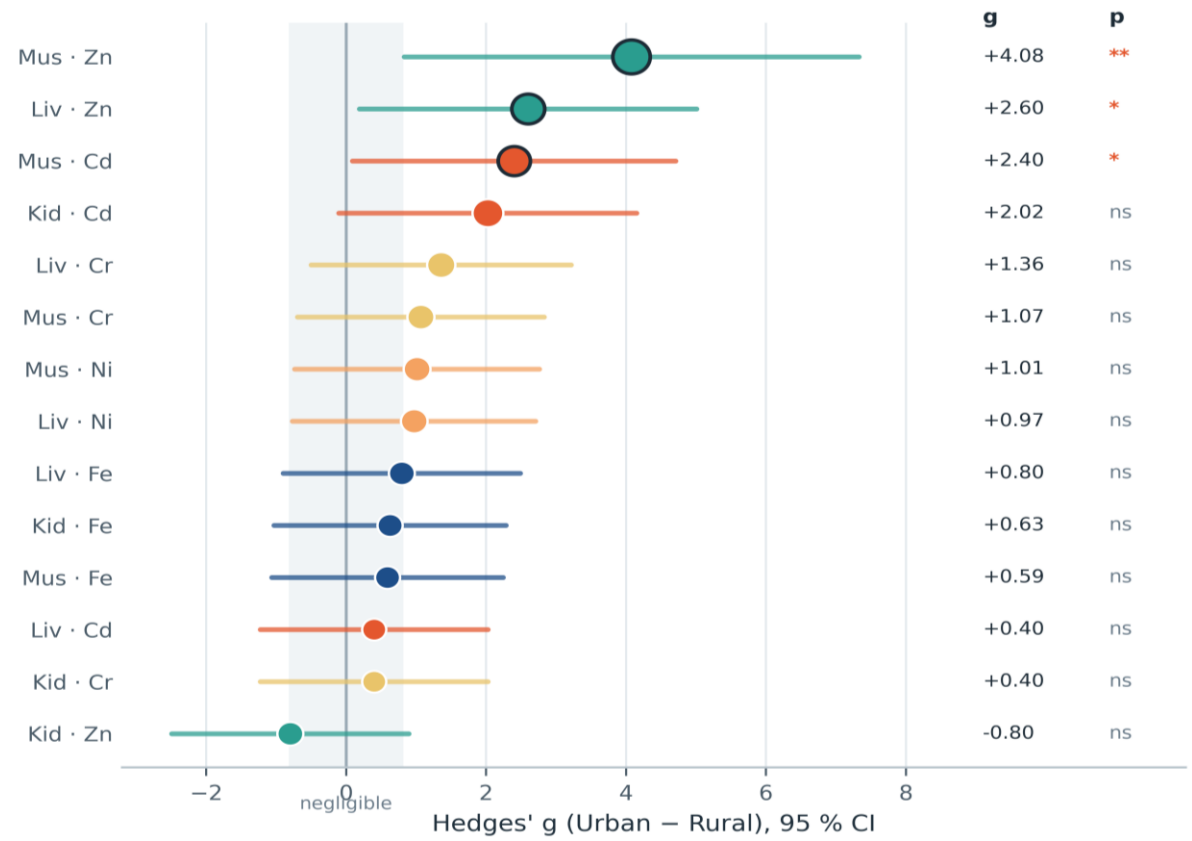


Figure 9: Forest plot of Hedges' g with 95 % confidence intervals for all fourteen contrasts.

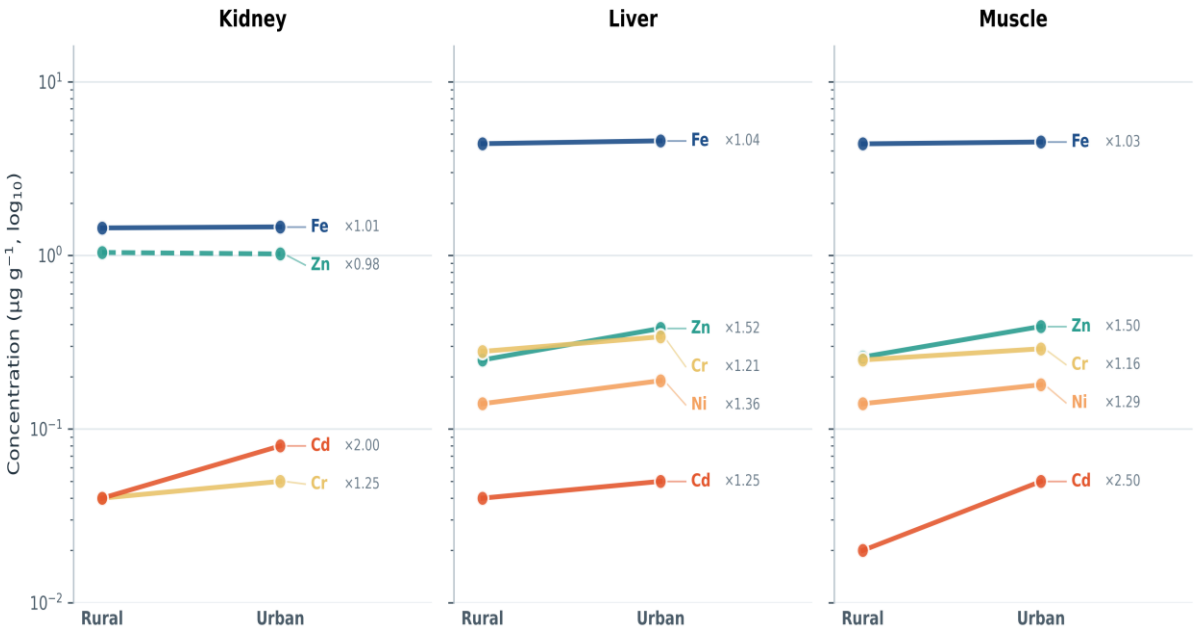


Figure 10: Slope plot showing the rural-to-urban trajectory of every quantified element, annotated with contamination factors.

3.5 Integrated contamination burden

The Metal Pollution Index rose from rural to urban in all three tissues (Figure 11): kidney 0.221 → 0.278 (+26 %), liver 0.280 → 0.355 (+27 %) and muscle 0.240 → 0.341 (+42 %). Muscle therefore showed the

largest integrated displacement despite containing no element at markedly elevated absolute concentration, because the index is sensitive to proportional change across the whole element suite rather than to any single high-abundance component. Ranked by integrated urban burden, liver (MPI = 0.355) exceeded muscle (0.341), which exceeded kidney (0.278).

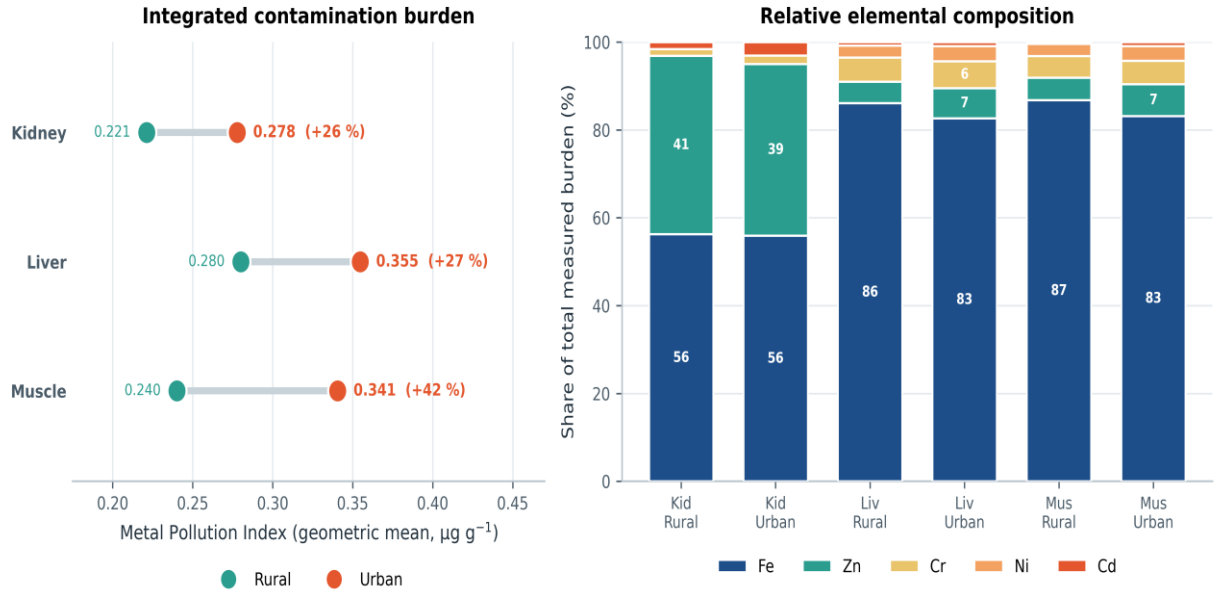


Figure 11: Left: Metal Pollution Index for each tissue, rural versus urban. Right: relative elemental composition of the total measured burden in each stratum.

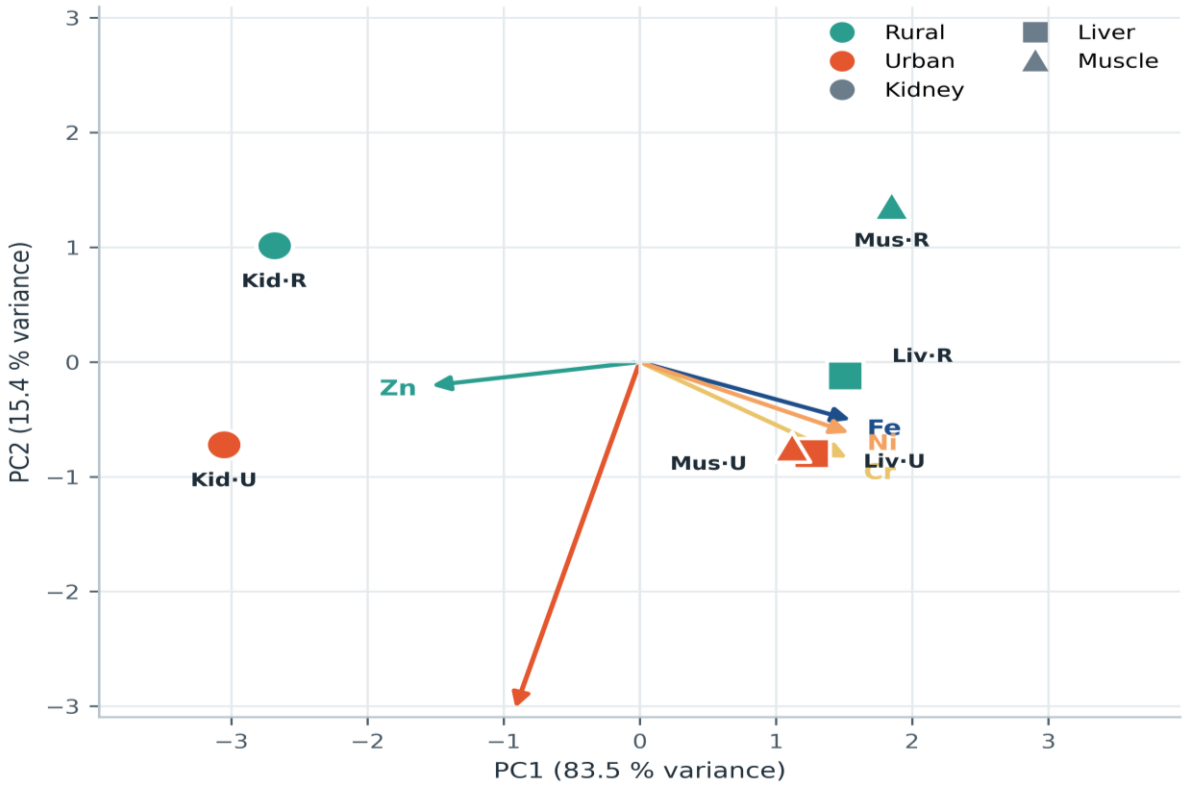


Figure 12: Principal component analysis biplot of the six tissue × site elemental profiles.

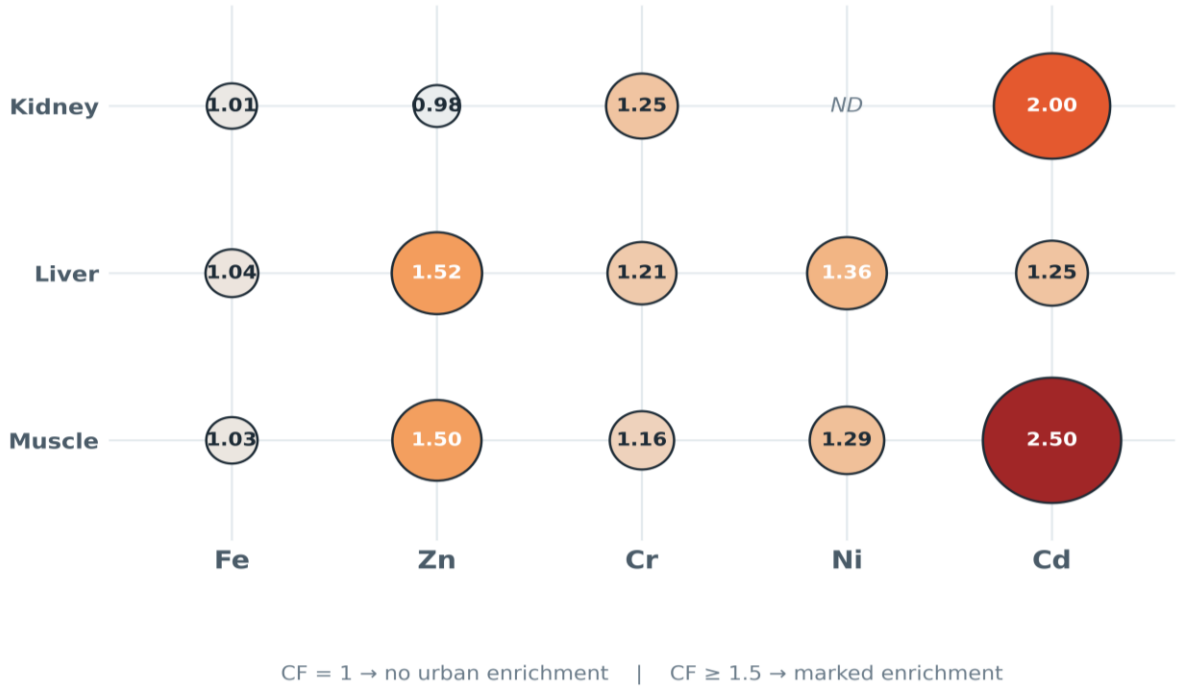


Figure 13: Contamination factor matrix; bubble area is proportional to urban enrichment.

3.6 Comparison with avian toxicity thresholds

To translate the measured burdens into ecological terms, we compared values against thresholds compiled for wild birds. The avian renal threshold indicating elevated environmental Cd exposure is 2–8 μg g^{-1}, and the hepatic threshold for Cd poisoning is 40 μg g^{-1} (Khwankitrittikul et al., 2024; Scheuhammer, 1987). Maximum kidney Cd observed here was 0.08 μg g^{-1} — between 25 and 100 times below the lower bound of the exposure-indicator range and maximum hepatic Cd was 0.05 μg g^{-1}, some three orders of magnitude below the poisoning threshold. Zinc, which becomes toxicologically relevant in avian tissue at concentrations two to three orders of magnitude above those recorded here, likewise remained far below any effect level. The measured burdens are therefore best interpreted as a **sub-toxic exposure signal**, not as evidence of metal poisoning. Their value lies in the consistency and structure of the rural–urban contrast rather than in the absolute magnitudes.

4. Discussion

The central result of this study is not any single significant contrast but the internal coherence of the pattern. Thirteen of fourteen quantifiable element × tissue comparisons moved in the same direction; the exception, kidney Zn, deviated by 2 %, which is within analytical repeatability. Directional concordance of this strength is unlikely under a null hypothesis of no habitat effect, and it accords with the wider literature on urban–rural contrasts in *P. domesticus*, beginning with Swaileh and Sansur (2006) and extended in the Moroccan series of Haddadi and colleagues, in which industrial and high-traffic strata consistently carried the highest Zn, Pb and Cd burdens and rural reference sites the lowest (Haddadi, Chahlaoui, Taouraout, Belkhiri, et al., 2024; Haddadi, Chahlaoui, Taouraout, Ichennarn, et al., 2025). More informative still is the *ordering* of enrichment. Contamination factors scaled inversely with biological essentiality: Cd (CF up to 2.50) > Zn in peripheral tissue (1.50–1.52) > Ni (1.29–1.36) > Cr (1.16–1.25) > Fe (1.01–1.04). Iron and renal zinc — the two elements under tight homeostatic control in vertebrates — were effectively invariant across the gradient, exactly as regulated elements should be. Cadmium and nickel, which have no physiological regulatory machinery, tracked the habitat contrast most strongly. This dissociation is difficult to explain by sampling artefact, digestion variability or instrumental drift, all of which would affect regulated and non-regulated elements alike. It is, however, precisely the signature

expected when an external, anthropogenic input is superimposed on a physiologically buffered baseline, and it substantially strengthens the case that the observed contrast is real.

Urban Okara concentrates several well-documented emission pathways. Cadmium in urban passerines is commonly attributed to vehicular sources — tyre and brake wear, lubricants and fuel combustion — together with the incineration and open dumping of household waste, batteries and plastics (Haddadi, Chahlaoui, Taouraout, Belkhiri, et al., 2024; Qu & Zheng, 2024). Nickel and chromium originate largely from alloy and steel working, electroplating, tanning and the metal-fabrication workshops typical of Pakistani urban commercial strips (Islam et al., 2022; Kumar et al., 2021). Zinc has both traffic-related sources, notably tyre wear and galvanised structures, and agricultural sources through fertiliser and feed supplementation, which may explain why the rural stratum recorded a comparable renal Zn burden to the urban stratum while its hepatic and muscular Zn remained lower (Haddadi, Chahlaoui, Taouraout, & Ichennarn, 2025). Iron's near-invariance is consistent with a large, ubiquitous crustal background against which incremental urban input is undetectable. The granivorous diet of the House Sparrow is the most likely exposure route. Seeds and grain gathered from roadside verges, refuse and market spillage in the urban stratum will carry deposited particulate metal, and granivorous birds have been shown to accumulate Cd in liver and kidney at higher rates than water birds from the same landscape, a difference attributed to feeding behaviour and to the ingestion of metal-contaminated seed (Khwankitrittikul et al., 2024). Incidental grit and soil ingestion during foraging provides a second route that is plausibly amplified in the dust-laden urban environment.

The accumulation hierarchies recovered here — Fe > Zn > Cd > Cr in kidney and Fe > Zn > Cr > Ni > Cd in liver and muscle — are consistent with the national feather survey of Abbasi et al. (2015), which reported an overall ranking of Fe > Zn > Cu > Pb > Mn > Cr > Ni > Co > Cd across 48 Pakistani bird species, and with the regional passerine baseline of Naz (2025). The clustering and PCA results add an important qualification: organ identity, not sampling site, is the dominant source of variance in the dataset (PC1, 83.5 %). Liver and kidney are the principal sites of metal metabolism, storage and detoxification, with high metallothionein expression and active transport machinery, and they therefore accumulate differently from skeletal muscle regardless of exposure (Mateo & Guitart, 2003; Yipel et al., 2023). That the habitat contrast nonetheless resolves on PC2 — loaded chiefly by Cd — demonstrates that the urban signal is detectable but secondary, and it argues strongly for multi-tissue sampling. A single-tissue design would have captured only part of the picture: kidney alone would have missed Ni entirely and understated Zn enrichment; muscle alone would have missed the renal Cd sequestration that is the classic signature of cadmium exposure. The finding that muscle showed the largest proportional MPI increase (+42 %) deserves comment. Muscle is not a primary detoxification organ and generally carries lower burdens, so a proportionally large rise there suggests that urban exposure is sufficient to exceed the buffering capacity of the hepatic and renal compartments and to spill into peripheral tissue. From an applied standpoint this also matters for human exposure, since muscle is the edible fraction in any avian species taken for consumption (Khan et al., 2023; Yacoubi et al., 2024).

A finding that distinguishes this analysis from the original draft is that the measured burdens lie far below published avian toxicity thresholds. Renal Cd of 0.08 μg g^{-1} is 25–100 times below the 2–8 μg g^{-1} range that flags elevated environmental Cd exposure in wild birds, and hepatic Cd of 0.05 μg g^{-1} is roughly three orders of magnitude below the 40 μg g^{-1} poisoning threshold (Khwankitrittikul et al., 2024; Scheuhammer, 1987). Claims that these concentrations exceed "permissible limits" cannot be supported without specifying the limit invoked and its provenance, and the present data do not indicate acute or chronic metal toxicosis in Okara sparrows. This does not diminish the result; it reframes it. Sub-toxic body burdens are exactly what a sensitive early-warning bioindicator should register. Sublethal exposure has nonetheless been associated with measurable biological cost in this species — morphometric change under elevated metal load (Albayrak & Pekgöz, 2021) and impairment of ecologically relevant behaviour at sublethal Pb (Di Liberto et al., 2024) — and metal stress may interact with the habitat loss, nest-site limitation, food scarcity, predation and disease pressures that jointly shape House Sparrow population trends. The appropriate conclusion is that Okara's urban environment imposes a detectable, sub-toxic and directionally consistent metal load on its resident sparrows, and that this load is rising with the district's urbanisation rather than that the birds are being poisoned.

4.5 Limitations

Several limitations constrain the interpretation of these findings. The principal limitation is the small sample size (n = 3 birds per stratum); at α = 0.05 and 80% power, this design can reliably detect only very large effects (Cohen's $d \approx 3.07$), making moderate but potentially ecologically important effects difficult to detect and explaining the occurrence of large effect sizes despite non-significant *p-values* and the absence of FDR-significant contrasts. Accordingly, interpret effect sizes and uncertainty alongside p values rather than treating statistical non-significance as evidence of no effect. Power calculations based on the observed effects suggest that approximately five birds per group would be required to detect the Cd–muscle effect ($g \approx 2.4$) and approximately 17 per group for the more modest Ni and Cr effects ($g \approx 1.0$) at 80% power. Spatial and temporal replication was also limited to one rural and one urban site sampled on a single occasion, preventing separation of habitat effects from site-specific characteristics and seasonal variation; future studies should therefore include multiple sites per stratum and repeated seasonal sampling. Important covariates, including sex, age, body mass, and body condition, were not modelled, although they may influence metal accumulation in passerines (Ding et al., 2023; Swaileh & Sansur, 2006). In addition, we did not analyse soil, water, dietary material, and airborne particulate matter concurrently, precluding estimation of environmental-to-tissue bioaccumulation relationships. The analytical scope was restricted to five elements, with lead a notable omission, and measurement of total chromium did not resolve the toxicologically relevant Cr(III)/Cr(VI) species; future work should therefore incorporate broader elemental profiling and chromium speciation (Iyer et al., 2023). Finally, because lethal tissue collection limits longitudinal monitoring, non-invasive matrices such as blood and feathers should be incorporated where appropriate; previous studies have demonstrated their utility for assessing Cd and Pb exposure and relating feather concentrations to internal tissue burdens (Coeurdassier et al., 2012; Bortolotti, 2010; Haddadi et al., 2025; Janaydeh et al., 2016; Manjula et al., 2015; Ding et al., 2023).

5. Conclusions and Future Directions

This study provides a tissue-resolved multi-element exposure profile of *Passer domesticus* in District Okara, Punjab, demonstrating tissue-specific accumulation patterns, consistently greater metal burdens in urban birds, and elevated integrated Metal Pollution Index values across kidney, liver, and muscle. The observed enrichment of Cd and Ni, contrasted with the relative stability of homeostatically regulated Fe, supports an external exposure signal, while the measured concentrations remained one to three orders of magnitude below established avian toxicity thresholds, indicating sub-toxic exposure rather than overt metal poisoning. Although several contrasts exhibited large effect sizes ($g > 0.8$), the absence of FDR-significant differences reflects the limited statistical power associated with n = 3 birds per group rather than definitive evidence of no biological effect. Future research should therefore prioritize adequately powered sampling with multiple rural and urban sites and repeated seasonal surveys, incorporate sex, age, body mass, and body condition as biological covariates, and analyse environmental matrices—including soil, water, dietary materials, and airborne particulates—to establish exposure pathways and bioaccumulation relationships. Expanded elemental profiling should include lead and other environmentally relevant metals, while chromium speciation should distinguish Cr(III) from Cr(VI) to improve toxicological interpretation. Longitudinal surveillance should additionally incorporate non-lethal matrices, particularly feathers and blood, to facilitate repeated biomonitoring while reducing reliance on destructive tissue collection. Collectively, these approaches would strengthen causal interpretation, improve spatial and temporal resolution of contamination patterns, and establish *P. domesticus* as a practical sentinel for monitoring bioavailable trace-metal exposure across rapidly urbanizing landscapes of central Punjab.

Declarations

Ethics. All procedures complied with institutional guidelines of the Department of Zoology, University of Okara.

Data availability. All data supporting the findings are contained in Tables 2 and 3 and the accompanying figures.

Funding. *N/A*

Conflicts of interest. The authors declare no competing interests.

REFERENCES

Abbasi, N. A., Jaspers, V. L. B., Chaudhry, M. J. I., Ali, S., & Malik, R. N. (2015). Influence of taxa, trophic level, and location on bioaccumulation of toxic metals in bird's feathers: A preliminary biomonitoring study using multiple bird species from Pakistan. *Chemosphere, 120*, 527–537. https://doi.org/10.1016/j.chemosphere.2014.08.054

Akram, M., Nawaz, Y., Nawaz, A., Munir, S., Riaz, H. F., Noreen, S., Shafi, M. T., Zaman, M., Wajid, M., Khan, M. S., Tanvir, F., & Riaz, S. (2024). Hematological variations and assessment of heavy metals in Sindh Sparrow (*Passer pyrrhonotus*) as a bioindicator in Punjab areas of Pakistan. *Journal of Advanced Zoology, 45*(2), 1451–1457. https://doi.org/10.53555/jaz.v45i2.3630

Albayrak, T., & Mor, F. (2011). Comparative tissue distribution of heavy metals in House Sparrow (*Passer domesticus*, Aves) in polluted and reference sites in Turkey. *Bulletin of Environmental Contamination and Toxicology, 87*(4), 457–462. https://doi.org/10.1007/s00128-011-0364-2

Albayrak, T., & Pekgöz, A. K. (2021). Heavy metal effects on bird morphometry: A case study on the House Sparrow *Passer domesticus*. *Chemosphere, 276*, 130056. https://doi.org/10.1016/j.chemosphere.2021.130056

Rather, M. A., Agarwal, D., Bhat, T. A., Khan, I. A., Zafar, I., Kumar, S., ... & Qadri, T. (2023). Bioinformatics approaches and big data analytics opportunities in improving fisheries and aquaculture. *International Journal of Biological Macromolecules*, *233*, 123549.

Aziz, B., Zubair, M., Irshad, N., Ahmad, K. S., Mahmood, M., Tahir, M. M., Shah, K. H., & Shaheen, A. (2021). Biomonitoring of toxic metals in feathers of birds from north-eastern Pakistan. *Bulletin of Environmental Contamination and Toxicology, 106*(5), 805–811. https://doi.org/10.1007/s00128-021-03184-w

Begum, W., Rai, S., Banerjee, S., Bhattacharjee, S., Mondal, M. H., Bhattarai, A., & Saha, B. (2022). A comprehensive review on the sources, essentiality and toxicological profile of nickel. *RSC Advances, 12*(15), 9139–9153. https://doi.org/10.1039/D2RA00378C

Benjamini, Y., & Hochberg, Y. (1995). Controlling the false discovery rate: A practical and powerful approach to multiple testing. *Journal of the Royal Statistical Society: Series B (Methodological), 57*(1), 289–300.

Bortolotti, G. R. (2010). Flaws and pitfalls in the chemical analysis of feathers: Bad news–good news for avian chemoecology and toxicology. *Ecological Applications, 20*(6), 1766–1774.

Coeurdassier, M., Fritsch, C., Faivre, B., Crini, N., & Scheifler, R. (2012). Partitioning of Cd and Pb in the blood of European blackbirds (*Turdus merula*) from a smelter contaminated site and use for biomonitoring. *Chemosphere, 87*(11), 1368–1373. https://doi.org/10.1016/j.chemosphere.2012.02.031

Cohen, J. (1988). *Statistical power analysis for the behavioral sciences* (2nd ed.). Lawrence Erlbaum Associates.

Di Liberto, J. F., Griffith, S. C., Hall, C. J., Mendelsohn, A. S., & Swaddle, J. P. (2024). Exposure to sublethal concentrations of lead (Pb) affects ecologically relevant behaviors in House Sparrows (*Passer domesticus*). *Archives of Environmental Contamination and Toxicology, 86*, 199–216. https://doi.org/10.1007/s00244-024-01062-0

Ding, J., Wang, S., Yang, W., Zhang, H., Yu, F., & Zhang, Y. (2023). Tissue distribution and association of heavy metal accumulation in a free-living resident passerine bird tree sparrow *Passer montanus*. *Environmental Pollution, 316*, 120547. https://doi.org/10.1016/j.envpol.2022.120547

Doccioli, C., Sera, F., Francavilla, A., Cupisti, A., & Biggeri, A. (2024). Association of cadmium environmental exposure with chronic kidney disease: A systematic review and meta-analysis. *Science of the Total Environment, 906*, 167165. https://doi.org/10.1016/j.scitotenv.2023.167165

Eens, M., Pinxten, R., Verheyen, R. F., Blust, R., & Bervoets, L. (1999). Great and blue tits as indicators of heavy metal contamination in terrestrial ecosystems. *Ecotoxicology and Environmental Safety, 44*(1), 81–85. https://doi.org/10.1006/eesa.1999.1828

Einhorn, V., Haase, H., & Maares, M. (2024). Interaction and competition for intestinal absorption by zinc, iron, copper, and manganese at the intestinal mucus layer. *Journal of Trace Elements in Medicine and Biology, 84*, 127459. https://doi.org/10.1016/j.jtemb.2024.127459

Fosmire, G. J. (1990). Zinc toxicity. *The American Journal of Clinical Nutrition, 51*(2), 225–227. https://doi.org/10.1093/ajcn/51.2.225

Government of the Punjab. (n.d.). *Geography – Okara*. Retrieved September 9, 2026, from https://okara.punjab.gov.pk/geography

Haddadi, Y., Chahlaoui, A., & Taouraout, A. (2025). Feathers of the House Sparrow (*Passer domesticus*) as a non-invasive tool for assessing urban and industrial metal pollution in Meknes, Morocco. *Bulletin of Environmental Contamination and Toxicology, 115*(6), 73. https://doi.org/10.1007/s00128-025-04142-6

Haddadi, Y., Chahlaoui, A., Taouraout, A., & Belkhiri, A. (2025). Assessing blood metal levels in House Sparrows (*Passer domesticus*) across urban and rural habitats in Meknes. *Environmental Science and Pollution Research, 32*(8), 4707–4717. https://doi.org/10.1007/s11356-025-35997-1

Haddadi, Y., Chahlaoui, A., Taouraout, A., & Ichennarn, I. (2025). Zinc bioaccumulation in House Sparrows (*Passer domesticus*) across urban and rural areas of Meknes, Morocco: A bioindicator of environmental pollution. *Environmental Monitoring and Assessment, 197*(4), 362. https://doi.org/10.1007/s10661-025-13772-6

Haddadi, Y., Chahlaoui, A., Taouraout, A., Belkhiri, A., & Ouballouk, Y. (2024). Cadmium accumulation in urban sparrows (*Passer domesticus*): Assessing the impact of high-traffic industrial areas in Meknes, Morocco. *International Journal of Environmental Studies, 81*(3), 1291–1309. https://doi.org/10.1080/00207233.2023.2287350

Haddadi, Y., Chahlaoui, A., Taouraout, A., Ichennarn, I., Jait, E., Saidi, A., Ouballouk, Y., & Belkhiri, A. (2025). Bioaccumulation of heavy metals in House Sparrow (*Passer domesticus*) kidneys across urban and rural habitats in Meknes, Morocco. *Journal of Experimental Zoology Part A: Ecological and Integrative Physiology, 343*(8), 846–856. https://doi.org/10.1002/jez.70001

Hashmi, M. Z., Malik, R. N., & Shahbaz, M. (2013). Heavy metals in eggshells of cattle egret (*Bubulcus ibis*) and little egret (*Egretta garzetta*) from the Punjab province, Pakistan. *Ecotoxicology and Environmental Safety, 89*, 158–165. https://doi.org/10.1016/j.ecoenv.2012.11.029

Hedges, L. V. (1981). Distribution theory for Glass's estimator of effect size and related estimators. *Journal of Educational Statistics, 6*(2), 107–128. https://doi.org/10.3102/10769986006002107

Helsel, D. R. (2012). *Statistics for censored environmental data using Minitab and R* (2nd ed.). John Wiley & Sons.

Iqbal, F., Wilson, R., Ayub, Q., Song, B. K., Krzeminska-Ahmedzai, U., Talei, A., Hermawan, A. A., & Rahman, S. (2023). Biomonitoring of heavy metals in the feathers of House crow (*Corvus splendens*) from some metropolitans of Asia and Africa. *Environmental Science and Pollution Research, 30*, 16736–16750. https://doi.org/10.1007/s11356-022-24712-z

Islam, S., Kamila, S., & Chattopadhyay, A. (2022). Toxic and carcinogenic effects of hexavalent chromium in mammalian cells in vivo and in vitro: A recent update. *Journal of Environmental Science and Health, Part C: Toxicology and Carcinogenesis, 40*(3–4), 282–315. https://doi.org/10.1080/26896583.2022.2158675

Iyer, M., Anand, U., Thiruvenkataswamy, S., Babu, H. W. S., Narayanasamy, A., Prajapati, V. K., Tiwari, C. K., Gopalakrishnan, A. V., Bontempi, E., Sonne, C., Barceló, D., & Vellingiri, B. (2023). A review of chromium (Cr) epigenetic toxicity and health hazards. *Science of the Total Environment, 882*, 163483. https://doi.org/10.1016/j.scitotenv.2023.163483

Janaydeh, M., Ismail, A., Zulkifli, S. Z., Bejo, M. H., Aziz, N. A., & Taneenah, A. (2016). The use of feather as an indicator for heavy metal contamination in House crow (*Corvus splendens*) in the Klang

area, Selangor, Malaysia. *Environmental Science and Pollution Research, 23*(21), 22059–22071. https://doi.org/10.1007/s11356-016-7223-y

Khan, B. N., Ullah, H., Ashfaq, Y., Hussain, N., Atique, U., Aziz, T., Alharbi, M., Albekairi, T. H., & Alasmari, A. F. (2023). Elucidating the effects of heavy metals contamination on vital organ of fish and migratory birds found at fresh water ecosystem. *Heliyon, 9*(11), e20968. https://doi.org/10.1016/j.heliyon.2023.e20968

Khwankitrittikul, P., Poapolathep, A., Poapolathep, S., Prasanwong, C., Kulprasertsri, S., & Khidkhan, K. (2024). Species differences and tissue distribution of heavy metal residues in wild birds. *Animals, 14*(2), 308. https://doi.org/10.3390/ani14020308

Kumar, A., Jigyasu, D. K., Kumar, A., Subrahmanyam, G., Mondal, R., Shabnam, A. A., Cabral-Pinto, M. M. S., Malyan, S. K., Chaturvedi, A. K., Gupta, D. K., Fagodiya, R. K., Khan, S. A., & Bhatia, A. (2021). Nickel in terrestrial biota: Comprehensive review on contamination, toxicity, tolerance and its remediation approaches. *Chemosphere, 275*, 129996. https://doi.org/10.1016/j.chemosphere.2021.129996

Malik, R. N., & Zeb, N. (2009). Assessment of environmental contamination using feathers of *Bubulcus ibis* L., as a biomonitor of heavy metal pollution, Pakistan. *Ecotoxicology, 18*(5), 522–536. https://doi.org/10.1007/s10646-009-0310-9

Manjula, M., Mohanraj, R., & Devi, M. P. (2015). Biomonitoring of heavy metals in feathers of eleven common bird species in urban and rural environments of Tiruchirappalli, India. *Environmental Monitoring and Assessment, 187*(5), 267. https://doi.org/10.1007/s10661-015-4502-x

Mateo, R., & Guitart, R. (2003). Heavy metals in livers of waterbirds from Spain. *Archives of Environmental Contamination and Toxicology, 44*(3), 398–404. https://doi.org/10.1007/s00244-002-2040-3

Maurya, P. K., Malik, D. S., Yadav, K. K., Kumar, A., Kumar, S., & Kamyab, H. (2019). Bioaccumulation and potential sources of heavy metal contamination in fish species in River Ganga basin: Possible human health risks evaluation. *Toxicology Reports, 6*, 472–481. https://doi.org/10.1016/j.toxrep.2019.05.012

National Institute of Standards and Technology. (n.d.). *Standard reference materials – SRM archive*. Retrieved September 9, 2026, from https://shop.nist.gov

Naz, R. (2025). Estimation of heavy metals toxicity of four passerines in the selected habitats of central Punjab, Pakistan. *International Journal of Agriculture and Biology, 33*(5), 330512. https://doi.org/10.17957/IJAB/15.2317

Ali, M. K., Javaid, S., Afzal, H., Zafar, I., Fayyaz, K., ul Ain, Q., ... & Sharma, R. (2023). Exploring the multifunctional roles of quantum dots for unlocking the future of biology and medicine. *Environmental Research*, *232*, 116290.

Oladimeji, T. E., Oyedemi, M. O., Odunfa, M. K., Agboola, O., Adeoye, J. B., Oke, M. A., & Akindele, O. O. (2025). From origin to oversight: Properties, impacts and management of heavy metals. *Discover Applied Sciences, 7*(11), 1353. https://doi.org/10.1007/s42452-025-07880-8

Özdemir, S., & Azizoğlu, E. (2025). Biomonitoring of heavy metals in the feathers of raptors from eastern Anatolia of Türkiye. *Frontiers in Ecology and Evolution, 13*, 1647589. https://doi.org/10.3389/fevo.2025.1647589

Panda, B. P., Parida, S. P., Pradhan, A., Mohanta, Y. K., Parthipan, P., Narayan, M., & Sarma, H. (2025). Identifying ecological risk zones using spatial prioritization of heavy metal pollution and bioaccumulation in birds. *Environmental Science and Pollution Research, 32*(18), 11727–11748. https://doi.org/10.1007/s11356-025-36385-5

Peana, M., Pelucelli, A., Chasapis, C. T., Perlepes, S. P., Bekiari, V., Medici, S., & Zoroddu, M. A. (2022). Biological effects of human exposure to environmental cadmium. *Biomolecules, 13*(1), 36. https://doi.org/10.3390/biom13010036

Qu, F., & Zheng, W. (2024). Cadmium exposure: Mechanisms and pathways of toxicity and implications for human health. *Toxics, 12*(6), 388. https://doi.org/10.3390/toxics12060388

Sarker, A., Kim, J.-E., Islam, A. R. M. T., Bilal, M., Rakib, M. R. J., Nandi, R., Rahman, M. M., & Islam, T. (2022). Heavy metals contamination and associated health risks in food webs — A review focuses

on food safety and environmental sustainability in Bangladesh. *Environmental Science and Pollution Research, 29*(3), 3230–3245. https://doi.org/10.1007/s11356-021-17153-7

Scheuhammer, A. M. (1987). The chronic toxicity of aluminium, cadmium, mercury, and lead in birds: A review. *Environmental Pollution, 46*(4), 263–295.

Swaileh, K. M., & Sansur, R. (2006). Monitoring urban heavy metal pollution using the House Sparrow (*Passer domesticus*). *Journal of Environmental Monitoring, 8*(1), 209–213.

Usero, J., González-Regalado, E., & Gracia, I. (1997). Trace metals in the bivalve molluscs *Ruditapes decussatus* and *Ruditapes philippinarum* from the Atlantic coast of southern Spain. *Environment International, 23*(3), 291–298. https://doi.org/10.1016/S0160-4120(97)00030-5

Welch, B. L. (1947). The generalization of "Student's" problem when several different population variances are involved. *Biometrika, 34*(1–2), 28–35. https://doi.org/10.1093/biomet/34.1-2.28

Wise, J. P., Young, J. L., Cai, J., & Cai, L. (2022). Current understanding of hexavalent chromium [Cr(VI)] neurotoxicity and new perspectives. *Environment International, 158*, 106877. https://doi.org/10.1016/j.envint.2021.106877

Yacoubi, L., Savoca, D., El Zrelli, R. B., Gopalan, J., Nazal, M., Lin, Y.-J., Maccotta, A., Hamza, F., Bhuyan, M. S., Arculeo, M., & Rabaoui, L. J. (2024). Trace element levels in the muscles of three tern species (Aves: Laridae) from the western Arabian Gulf: Environmental assessment and implications for conservation. *Environmental Monitoring and Assessment, 196*(3), 235. https://doi.org/10.1007/s10661-024-12385-9

Yipel, M., Tekeli, İ. O., İşler, C. T., & Altuğ, M. E. (2023). Tissue distribution and correlations of heavy metals in wild birds from southern Turkey: An ecologically important region on the west Palearctic migration route. *Environmental Science and Pollution Research, 30*(26), 68889–68899. https://doi.org/10.1007/s11356-023-27292-8

Zhang, H., Zhao, Y., Wang, Z., & Liu, Y. (2021). Distribution characteristics, bioaccumulation and trophic transfer of heavy metals in the food web of grassland ecosystems. *Chemosphere, 278*, 130407. https://doi.org/10.1016/j.chemosphere.2021.130407

Zhou, Q., Zhang, J., Fu, J., Shi, J., & Jiang, G. (2008). Biomonitoring: An appealing tool for assessment of metal pollution in the aquatic ecosystem. *Analytica Chimica Acta, 606*(2), 135–150. https://doi.org/10.1016/j.aca.2007.11.018